

**This item is the archived peer-reviewed author-version of:**

Electrochemical analysis of cocaine in real samples based on electrodeposited biomimetic affinity ligands

**Reference:**

Florea Anca, Cow en Todd, Piletsky Sergey, De Wael Karolien.- Electrochemical analysis of cocaine in real samples based on electrodeposited biomimetic affinity ligands  
The analyst - ISSN 0003-2654 - 144:15(2019), p. 4639-4646  
Full text (Publisher's DOI): <https://doi.org/10.1039/C9AN00618D>  
To cite this reference: <https://hdl.handle.net/10067/1600620151162165141>



## Electrochemical sensing of cocaine in real samples based on electrodeposited biomimetic affinity ligands

Anca Florea<sup>a</sup>, Todd Cowen<sup>b</sup>, Sergey Piletsky<sup>b</sup>, Karolien De Wael<sup>a\*</sup>

AReceived 00th January 20xx,  
Accepted 00th January 20xx

DOI: 10.1039/x0xx00000x

[www.rsc.org/](http://www.rsc.org/)

A selective electrochemical sensor for direct detection of cocaine was developed based on molecularly imprinted polymers electropolymerized onto graphene-modified electrodes. Palladium nanoparticles were integrated in the sensing layer for the benefit of enhancing the communication between imprinted sites and electrode and improving their homogenous distribution. The molecularly imprinted polymer was synthesized by cyclic voltammetry using *p*-aminobenzoic acid as high affinity monomer selected by computational modeling, and cocaine as template molecule. Experimental parameters related to the electrochemical deposition of palladium nanoparticles, pH, composition of electropolymerization mixture, extraction and rebinding condition were studied and optimized. Under optimized conditions the oxidation peak current varied linearly with cocaine concentration in the range of 100–500  $\mu\text{M}$ , with a detection limit of 50  $\mu\text{M}$  (RSD 0.71%,  $n=3$ ). The molecularly imprinted sensor was able to detect cocaine in saliva and river water with good recoveries after sample pretreatment and was successfully applied for screening real street samples for cocaine.

### Introduction

Illicit drugs use and abuse is a major problem in the contemporary society. Cocaine is Europe's most commonly used illicit stimulant drug with a retail market worth at least 5.7 billion euros per year. The health harms related with regular cocaine consumption, whether as cocaine powder or crack, include addiction, kidney damage, respiratory, heart and mental health problems. Even though deaths associated with cocaine are likely to be underestimated, being attributed to other conditions, over 800 deaths related to drug overdose were reported in 2013 in Europe<sup>1</sup>. To control this serious global public health problem an accurate, easy-to-use and low cost point-of-use cocaine test is of interest for public authorities to quickly detect cocaine at borders, workplaces or on the roadside.

The conventional methods for cocaine detection include high performance liquid chromatography and mass spectrometry<sup>2,3</sup>. Despite their accuracy and reliability, these methods are time- and cost-consuming, require trained personnel and complex sample pretreatment, and are less suitable for miniaturization for on-site measurements. Thus, there is a need for developing accurate, low-cost sensing devices that can be employed on-site for fast drug detection and identification. Electrochemical sensing of cocaine attracted much interest from the research community lately<sup>4,5</sup>, with over 90% of papers on this topic being published in the past 12 years according to a recent review by Poltorak et al<sup>6</sup>. The review

exhaustedly describes advances made for cocaine electrochemical detection at bare and modified electrodes (apta-, immuno- and enzymatic sensors), soft junctions and nanopore sensing. One of the first study on the electrochemical behavior of cocaine at bare electrodes was reported by Fernandez Abedul et al<sup>7</sup>, and applied on confiscated samples analysis in solution. Komorsky-Lavric et al<sup>8</sup> demonstrated the possibility to detect cocaine in powder form at paraffin-impregnated electrodes without dissolving the sample, but the effect of adulterants has not been studied. Asturias-Arribas et al<sup>9</sup> employed disposable electrodes to detect cocaine in solution in the presence of adulterants, such as codeine, caffeine and paracetamol, using a statistical regression method to overcome interferences. Our group developed strategies for detecting cocaine both in solution and powder in the presence of several major cutting agents using screen-printed electrode systems and noticeable interference was found for a number of adulterants<sup>10–12</sup>, hence the need for more selective detection strategies. In addition to confiscated samples analysis, electrochemical techniques have been employed also for the detection of cocaine in various biological samples such as urine, saliva or blood, most of which are based on aptamers<sup>13–19</sup>. Aptamers are affinity ligands conferring high selectivity of detection and low detection limits<sup>20,21</sup>, however they may suffer some instability issues when used in extreme and even ambient conditions (e.g. pH, temperature, ionic strength and prolonged storage). Molecularly imprinted polymers (MIPs) are synthetic biomimetic materials tailor-designed to specifically bind the molecule of interest with high affinity. Being more robust than aptamers MIPs may overcome the stability issues. Recently, a great deal of work was focused on the integration of MIP nanoparticles (including cocaine imprinted polymers) with electrochemical transducers<sup>21</sup>. For example, Piletsky's group developed a potentiometric sensor for cocaine based on imprinted nanoparticles chemically prepared<sup>22</sup>. The sensor described in this work however required electrochemical cell and

<sup>a</sup> University of Antwerp, Department of Chemistry, Groenenborgerlaan 171, B-2020, Belgium

<sup>b</sup> University of Leicester, Department of Chemistry, LE1 7RH, UK

\* Corresponding author, E-mail address: karolien.dewael@uantwerpen.be

† Footnotes relating to the title and/or authors should appear here.

Electronic Supplementary Information (ESI) available: [details of any supplementary information available should be included here]. See DOI: 10.1039/x0xx00000x

was not suitable for roadside tests. An easy route to produce portable sensor is direct electropolymerization of MIPs on the surface of screen-printed electrode, which gives the advantage of controlling film thickness and obtaining thin films with accessible binding sites that intimately adhere to the electrode surface; also it is less time- and solvent-consuming ("green") protocol compared to other methods of preparing MIPs. Experimental screening in the laboratory to find the best combination of template and functional monomer can be tedious, but the work load can be considerably reduced by using computational techniques, which can narrow down the search to a few optimum combinations that can then be empirically tested in the laboratory<sup>23</sup>. Computational design has proved to be an effective tool in MIP preparation to screen for functional monomers, giving information on the type and intensity of monomer-template interaction, for ratio optimization, and for binding site interactions analyses<sup>24-30</sup>.

In order to apply MIPs in sensors, several parameters should be improved such as their binding kinetics, analysis times, and assuring complete removal of the template<sup>31-33</sup>. The integration of nanomaterials into sensing layers can overcome these challenges by enhancing the sensor surface area, leading to an increase in MIPs sensitivity. Nanomaterials can remarkably increase the intensity of electrochemical signals derived from accumulation of large amounts of electroactive analytes at electrode surfaces<sup>22,34</sup>. The synergistic effect of graphene (GPH) and metallic particles was exploited in several electrochemical sensors based on MIPs. For example, graphene/gold nanoparticles (AuNPs) composites were integrated with MIPs sensors and applied for the detection of carbofuran<sup>35</sup>, levofloxacin<sup>36</sup> or chloramphenicol<sup>37</sup>. Their integration led to an increased specific surface area, enhanced electrochemical signal and a high adsorption capability, which allowed reaching detection limits in the order of magnitude of  $10^{-7}$ - $10^{-8}$  M.

In this work, an electrochemical sensor was developed for the selective detection of cocaine based on electrodeposited MIPs and palladium nanoparticles (PdNPs) onto GPH-functionalized electrodes. MIP layers with specific recognition properties for cocaine were readily prepared by cyclic voltammetry (CV) using *p*-aminobenzoic acid (PABA) as monomer and cocaine as template molecule. The monomer was selected by computational techniques. The experimental conditions that have an influence on the performance of the sensor were studied and optimized such as pH, monomer:template ratio, number of electropolymerization cycles, extraction solution, extraction and rebinding time. The sensor was applied for the detection of cocaine in various matrices such as street samples, saliva and river water after a dilution step. To the best of our knowledge the fabrication of an amperometric sensor based on electropolymerized MIPs for cocaine direct detection has not been previously reported.

## Experimental

### Reagents

Cocaine hydrochloride was obtained from Lipomed (Arllesheim, Switzerland). Palladium chloride, *p*-aminobenzoic acid (PABA), potassium monophosphate, potassium chloride, potassium hydroxide and concentrated sulfuric acid were purchased from Sigma-Aldrich (Overijse, Belgium). Phosphate buffer saline 20 mM

containing 100 mM KCl (PBS) was used throughout the experiments and the pH was adjusted to the desired value with NaOH solution. Stock solutions of cocaine with a concentration of 50 mM in MilliQ water were prepared and stored in the fridge. PABA solutions were prepared in PBS pH 7.0 and kept in the fridge for up to 3 days. All reagents were of analytical grade. All aqueous solutions were prepared using MilliQ water ( $R > 18 \text{ M}\Omega\text{cm}$ ).

Saliva collection devices from Quantisal (The Netherlands) were used for saliva analysis. Saliva was collected according to package instruction and diluted 1:10 in PBS pH 7.0. The sample was then spiked with various concentrations of cocaine and subjected to electrochemical measurements.

River water samples were collected from Schelde river in Antwerp. The samples were subjected to filtration through a disposable syringe filter with pore size 0.45  $\mu\text{m}$  (Chromafil® AO-45/25) diluted 1:10 in PBS pH 7.0 and spiked with cocaine.

Cocaine street samples were provided by National Institute of Criminalistics and Criminology (NICC), Belgium, with the following composition determined by gas chromatography coupled with mass spectrometry (GC-MS): sample 1, 19.2% cocaine, 73.2% paracetamol, 1.6% levamisole; sample 2, 31% cocaine, 2.8% phenacetine, 5.7% levamisole, mannitol. The GC-MS analysis (HP6890N-5973N, Agilent Technologies, Santa Clara, CA, USA) was performed for identification, based on comparison with in-house libraries (retention time and spectra) as previously described by Eliaerts et al<sup>38</sup>. An Agilent DB5-MS column (15.0 m  $\times$  250  $\mu\text{m}$   $\times$  0.25  $\mu\text{m}$ ) was used with helium as carrier gas at constant pressure with retention time locking. The oven temperature was initially set as 100°C and then increased to 325°C. A volume of 1  $\mu\text{L}$  was injected in the split mode with a split ratio of 40:1. The run time was 14.25 min. MSD Chemstation software (Agilent Technologies, Santa Clara, CA, USA) was used for data retrieval.

For street samples analysis with the electrochemical sensor 1 mg street sample powder was dissolved in 1 mL PBS pH 7.0. The solution was then diluted 1:1 with PBS pH 7.0 and used for screening with electrochemical methods.

### Instrumentation and measurements

The computational modelling was conducted as described previously by Piletsky's group<sup>22</sup>. A screening of a virtual library of electropolymerizable monomers was done to check their interaction with the template using LEAPFROG™ algorithm (SYBYL® 7.3 software package, Tripos International, USA). Energy minimization was performed to a minimum of 0.001 kcal mol<sup>-1</sup>. The parameters of molecular mechanics were: method - Powell, force field - Tripos and charges - Gasteiger-Huckel. The monomers were ordered by the relative binding energy.

All electrochemical measurements were performed with Autolab potentiostat/galvanostat (PGSTAT 302N, ECOCHÉMIE, The Netherlands) controlled by NOVA software. Graphite screen-printed electrodes modified with graphene (GPH-SPE) consisting of a working electrode (3 mm diameter), a carbon counter electrode and a (pseudo)silver reference electrode were purchased from DropSens (Spain). PdNPs were electrodeposited at the surface of the working electrode from a solution of palladium chloride 2 mM in 0.1 M sulfuric acid by applying a fixed potential of -0.14 V for 120s. Electropolymerization of MIP was performed by cyclic voltammetry

(CV), sweeping the potential between -0.5 to 1.0 V, at a scan rate 50 mV/s, for 10 cycles, in a 100  $\mu$ L drop of PBS pH 7 solution containing PABA as monomer and cocaine as template. NIP was prepared as control in a similar manner as MIP without any addition of template. Square wave voltammetry (SWV) was performed in the potential range 0.3-1.1 V, with a step potential of 5 mV, an amplitude of 25 mV, a frequency of 10 Hz, in PBS pH 11.0 solution. SWV was employed to characterize the sensor in different steps of the fabrication, in a drop of 100  $\mu$ L PBS pH 11.0 solution placed on the surface of the electrodes. Cocaine rebinding experiments were ran by placing a drop of 100  $\mu$ L analyte solution on the electrodes for the uptake of cocaine. Afterwards, the drop was removed and 100  $\mu$ L PBS pH 7.0 was placed onto the electrode and left for 1 min to wash weakly adsorbed analytes. Finally, 100  $\mu$ L PBS pH 11.0 was placed onto the electrode and SWV was run. All results obtained by SWV were presented after baseline correction using the mathematical algorithm "moving average" (peak width = 1) contained within NOVA software, to improve the visualization and identification of the peaks over the baseline. All electrochemical experiments were performed at room temperature.

GPH-SPE modified with PdNPs were examined with a Field Emission Gun – Environmental Scanning Electron Microscope (FEG-ESEM) equipped with an Energy Dispersive X-Ray (EDX) detector (FEI Quanta 250, USA; University of Antwerp), using an accelerating voltage of 20kV, a take-off angle of 30°, a working distance of 10 mm and a sample chamber pressure of 10<sup>-4</sup> Pa. Imaging was performed based upon secondary electrons, back-scattered electrons.

## Results and discussions

### Electrochemical fabrication of MIP sensor

Electropolymerization allows simple, controlled deposition of thin films at the surface of electrodes<sup>39</sup> as opposed to bulk polymerization techniques for MIP preparation. The protocol for MIP fabrication is presented in Figure 1.

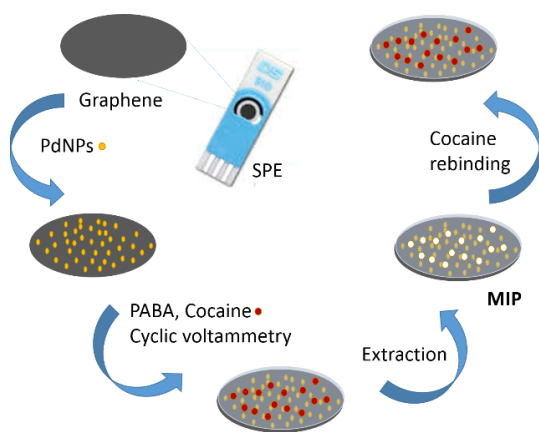


**Figure 1.** Schematic illustration of the electrochemical fabrication of MIP sensor for cocaine

In the first step PdNPs were readily deposited onto the surface of GPH-SPE by potentiostatic methods. GPH was shown to increase the conductivity and electropolymerization rate of PABA films<sup>40</sup>, while metal nanoparticles integrated in MIP layers were shown to enhance the number of accessible imprinted sites and improve their homogenous distribution, and to provide surface with catalytic activity<sup>41</sup>. Scanning electron microscopy (SEM) image confirmed the electrodeposition of PdNPs at GPH-modified SPE with mean diameter of 70 nm (Figure 2). In general, nanoparticles (NPs) are preferentially deposited on the substrate defects or at the edges, resulting in a less uniform distribution<sup>42</sup>.

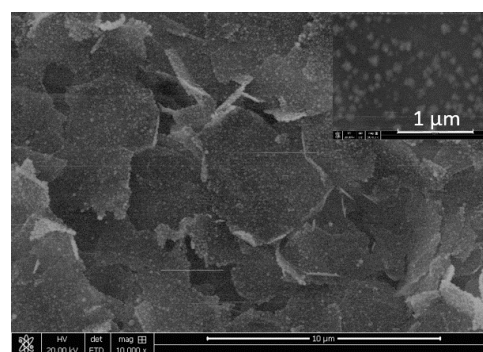


**Figure 2.** SEM observation of PdNPs@GPH-SPE

In the next step, MIP-films were electrodeposited directly onto the electrodes by CV. The electropolymerization was carried out in PBS solution at pH 7.0 containing 4 mM PABA as functional monomer and 1 mM cocaine as template molecule by sweeping the potential between -0.5 to 1.0 V, at a scan rate of 50 mV/s, for 10 cycles. PABA was selected as suitable functional monomer for MIP fabrication as it exhibits high binding affinity for cocaine according to the results of computational modelling (binding score -114.99 kJ mol<sup>-1</sup>, Table S1, Supplementary Information). The hydrogen bonding between the hydrogen of the amine in the aminogroup of PABA and the carbonyl of the benzoylmoiety in cocaine (Figure 3) promote the embedding of cocaine in the polymer matrix.

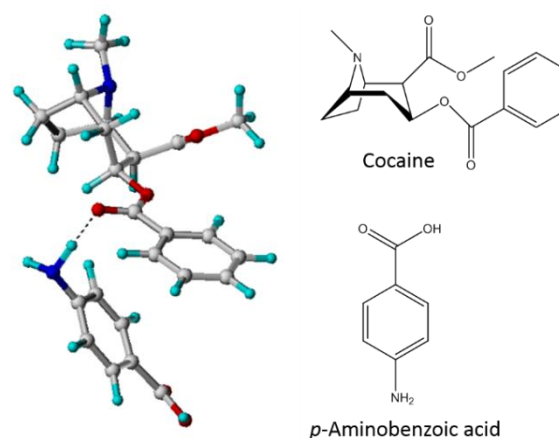


**Figure 3.** Modelling of cocaine-PABA interaction

Non-imprinted films (NIP) were prepared in a similar manner but without the addition of the template in the polymerization step and used as a control. Figure 4 shows the cyclic voltammogram for the electropolymerization of MIP (Figure 4A) and NIP (Figure 4B). A distinct and irreversible peak appears in the first cycle around 0.70 V, related to the oxidation of the monomer, which decreases with each polymerization cycle as the monomer is consumed and the electrode surface is passivated during film growth. A shoulder is present at 0.63 V for NIP in comparison with MIP, showing that the presence of cocaine may have an effect on the oxidation of the monomer, however the influence is not significant as shown by the similar behavior in the following CV cycles. A pair of anodic and cathodic peaks arise after the first cycle at around 0.15 V and 0 V, respectively, that increase gradually after each polymerization cycle showing the growth of the polymeric film. A reduction peak appears at around -0.14 V for both MIP and NIP, which can be attributed to the reduction of Pd<sup>2+</sup> formed during the oxidation sweep to Pd<sup>0</sup>. The peak intensity is increasing in the first three electropolymerization cycles and then the peak disappears the PdNPs being partly covered by the polymer layer.

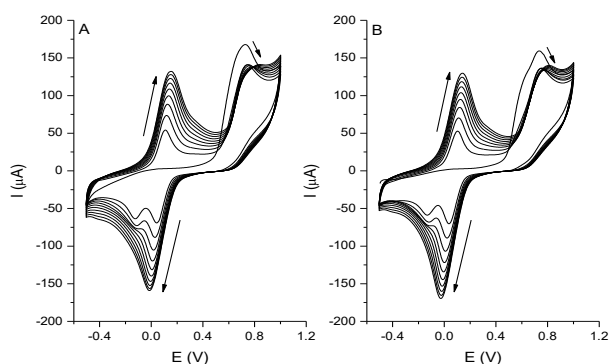


**Figure 4.** Cyclic voltammograms for electropolymerization of MIP (A) and NIP (B). Parameters: potential range -0.5-1V, scan rate 50 mV/s, 10 cycles; PABA concentration 4 mM; cocaine concentration 1 mM; electrolyte PBS pH 7.0.

In the final step template is removed from the polymer matrix, forming surface imprinted sites capable of selective recognition and binding cocaine. For the removal of the template 100  $\mu\text{L}$  extraction solution was placed onto the modified SPE and let in contact for various time frames. The effective removal of cocaine from the MIP layer was checked by performing SWV before and after extraction. Figure 5 shows the presence of an oxidation peak for cocaine at 0.88 V after MIP electropolymerization due to the entrapment of cocaine inside the MIP film. The signal disappears after the extraction step. For the NIP film no signal was observed for cocaine after electro polymerization, since cocaine was not added to the polymerization mixture. This behavior is an indication for the formation of cavities in the MIP film, templated by the size and shape of cocaine.

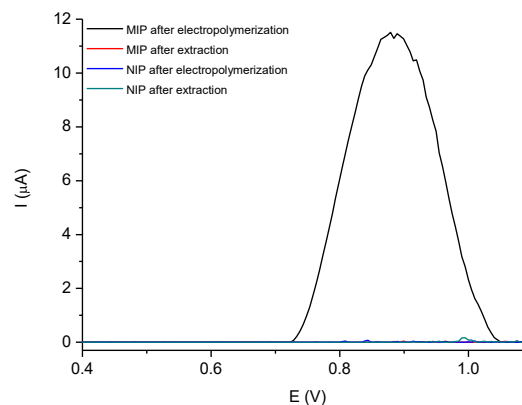


**Figure 5.** SWV at MIP and NIP films after electropolymerization and after extraction, in PBS pH 11.0. Scan rate 50 mV/s. Note that the curves related to MIP after extraction, NIP after electropolymerization and NIP after extraction are overlaid.

### Optimization

Several parameters related to the deposition of PdNPs, electropolymerization of MIP, extraction solution and time, rebinding time and detection solution were optimized to achieve the best performance of MIP sensors. To choose the optimal conditions, the imprinting factor (IF) was evaluated for each parameter. For this purpose, the SWV response of the MIP and NIP modified electrodes to the cocaine was appraised and compared: the modified electrodes were incubated with cocaine solutions of concentrations in the range of 100-500  $\mu\text{M}$  for 10 minutes, washed to remove non-specifically bound molecules and subjected to SWV measurements in PBS pH 11.0. A calibration curve was obtained in each case for both MIP and NIP. The IF was calculated as the ratio of the slope of MIP and the slope of NIP as a measure of cocaine retention.

### Deposition of PdNPs and pH

The first step in the fabrication of the sensor consists in the electrodeposition of PdNPs. The size and size distribution of NPs are the most important features influencing their performance in electrochemical sensor design, because depending on the size and the distance between adjacent particles, the degree of diffusion-layer overlap (the nature of the voltammetric responses) can be manipulated. By applying a reducing potential, NPs are directly electrodeposited from the appropriate salt solutions onto the electrode surface in the desired format. The electrodeposition of NPs is a facile manner of surface modification, although control of the size of the particles may be greatly dependent on deposition time, applied potential, electrolyte solution, and the salt concentration<sup>43</sup>. To improve the sensor performance, palladium (Pd) was deposited at GPH-SPE from aqueous solutions of 2 mM PdCl<sub>2</sub> in 0.1 M H<sub>2</sub>SO<sub>4</sub> by applying a fixed potential of -0.14 V for a certain period of time. The behaviour of PdNPs at different pH values was firstly evaluated, to assess if any signal appears that could overlap the SWV signal of cocaine and thus interfere with its detection. For this, PdNPs were grown under potentiostatic conditions for 240 sec and SWV was performed in solutions of PBS pH 7.0-12.0 at the Pd-modified electrodes (Figure 6A). In another set of experiments, a layer of

polyPABA (NIP) was electrodeposited onto Pd@GPH-SPE prior to running SWV measurements in PBS solution pH 7.0–12.0, to check the behaviour of Pd/polymer layer in different pH conditions (Figure 6B). It was observed that at pH 7.0–9.0 and pH 12.0 oxidation peaks appear in the potential range of interest (around 0.85 V) on Pd-modified electrodes. When the electrodes are covered with a layer of polyPABA, these peaks are considerably reduced, however the presence of substantially high signals at pH 12.0 may interfere with cocaine detection, thus pH 12.0 was avoided in following experiments. Correlating these finding with the fact that cocaine exhibits enhanced oxidation signals at higher pH values<sup>9</sup>, PBS buffer with pH 11.0 was selected for the detection step. Moreover, at pH 11.0 cocaine is neutral and it assures low non-specific binding. The deposition time of PdNPs was optimized by varying the time between 30 sec and 240 sec. The electrodes were then covered with MIP and NIP layers as described in section 1, using 7 electropolymerization cycles, and the response of MIP versus NIP toward cocaine binding (IF) was evaluated. The highest IF and the best correlation factor for MIP was obtained for 60 sec deposition time (IF 1.64,  $R^2$  0.996) which was further selected for the following experiments. For 30 sec deposition time an IF of 1.42 and a correlation factor for MIP of 0.952 was obtained. For 120 sec and 240 sec, the IF was 1.04 and 1.16 and the correlation factor for MIP of 0.972 and 0.993, respectively.

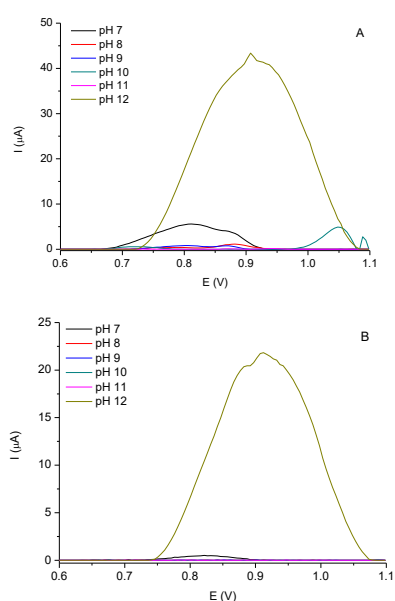


**Figure 6.** SWV at Pd@GPH-SPE (A) and Pd/polyPABA@GPH-SPE films (B) in PBS pH 7.0–12.0. Scan rate 50 mV/s. Note that the curves related to pH 8.0–11.0 (B) are overlaid.

#### Number of electropolymerization cycles and monomer:template ratio

An optimization study of the ratio of the monomer to template and their concentrations was conducted. The number of electropolymerization cycles was also tuned, since it is an important parameter correlated to the film thickness and morphology. The results are presented in table 1. In a first set of experiments, the

concentration of the monomer was varied, while the cocaine concentration was kept constant at 1 mM. Seven electropolymerization cycles were performed. The highest sensitivity for MIP was achieved for 4:1 ratio. Although a good IF was obtained for a 6:1 ratio the sensitivity of both MIP and NIP for cocaine was low, with MIP slope 0.009 compared to NIP slope 0.003, probably due to lower accessibility of cocaine to the binding sites due to higher film thickness and lower film conductivity. Thus the 4:1 ratio was selected and further optimized. Keeping the monomer:template ratio fixed at 4:1, the number of electropolymerization cycles was further increased to 10 cycles. An increase of both the IF (2.1) and MIP slope (0.021) was observed compared to 7 cycles. Further increasing the number of cycles to 15 did not result in an increased performance of the sensor probably due to the higher film thickness and poorer accessibility of cocaine to the binding sites. Further on, keeping the concentration of the monomer fixed at 4 mM and the number of cycles at 10, the concentration of the template was varied, maintaining the monomer:template ratios of 3:1, 4:1, 5:1, 6:1 and 7:1. The maximum imprinting was obtained for concentrations of 4 mM PABA to 1 mM cocaine, therefore these conditions were employed in further experiments.

**Table 1** Optimization of number of cycles and monomer:template ratio and concentrations

Cycles of electropolymerization	Monomer:template ratio	IF
7	2:1	1.5
	3:1	1.1
	4:1	1.55
	5:1	1.5
	6:1	2.9
	7:1	0.75
10	4:1	2.1
15	4:1	1.63
10	4:0.75	0.8
	4:1.25	1.24
	4:1.5	0.97
	4:1.75	0.91

#### Extraction solution, extraction and rebinding time

Efficient extraction of the template molecules from the polymer matrix is an essential step in MIP synthesis. Several extraction solutions were tested for this purpose, taking into consideration the solubility of cocaine in different solvents (Table 2). For this purpose 100  $\mu$ L extraction solution was placed onto the electrode and left for a certain time. Afterwards, the electrode was rinsed with double distilled water and SWV measurements were performed in PBS pH 11.0 to assess the disappearance of cocaine peak. Given the higher solubility of cocaine in acetone, as well as the instability of GPH-electrodes ink in acetone, the extraction with water/acetone mixture was not performed for a time longer than 10 min. After 10 min extraction the cocaine peak has disappeared completely. After template extraction, cocaine rebinding experiments were performed for both MIP and NIP as previously described in section 2, comparing the IF of MIP and NIP. The highest IF was obtained in case of

extraction with PBS pH 7.0 for 1h30, thus these conditions were selected for further experiments.

**Table 2** Optimization washing solution and time

Washing solution	Washing time	IF
Warm water	1h30	0.52
PBS pH 10.0	1h30	1.5
Water/ethanol 30%	1h30	1
Water	1h30	1.16
Water	1h	1.06
PBS pH 7.0	1h30	2.8
Water/acetone 20%	10 min	1
Water/acetone 10%	10 min	0.6

The effect of the rebinding time on the SWV peak intensity was further studied and optimized as described in Experimental section. As showed in Figure 7, the cocaine peak current increases as the time increases up to 5 min, as cocaine gradually accumulates in the binding sites, and then tends to level off, as saturation of the sites is obtained. Five minutes was selected as optimum incubation time with cocaine solution since the increase in the peak current is not significant after 5 min.

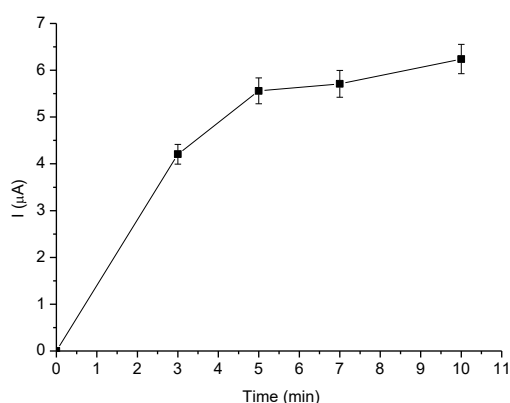


**Figure 7.** Optimization of rebinding time of cocaine solution 300  $\mu\text{M}$  in PBS pH 7.0 by MIP-modified electrodes ( $n=3$ )

Thus, the optimum conditions considered for further experiments were: monomer:template ratio and concentrations 4 mM :1 mM in PBS pH 7.0, extraction 1h30 with PBS pH 7.0, incubation time 5 min, measuring solution PBS pH 11.0.

#### Performance of MIP sensors for cocaine analysis

The developed sensor was used for the determination of cocaine at different concentrations under optimized conditions. SWV was employed for cocaine quantification. The obtained voltammograms, as well as the dependency of peak current versus concentration are shown in Figure 8. The current response varies linearly with the concentration of cocaine in the range of 100-500  $\mu\text{M}$ . The linear regression equations are expressed as  $I(\mu\text{A}) = 0.016C(\mu\text{M}) + 1.053$  with  $R^2 = 0.983$  for MIP and  $I(\mu\text{A}) = 0.05C(\mu\text{M}) + 0.15$  with  $R^2 = 0.946$  for NIP. The lowest concentration that could be detected with the MIP-sensor by SWV measurements was 50  $\mu\text{M}$  (%RSD 0.71,  $n=3$ ).

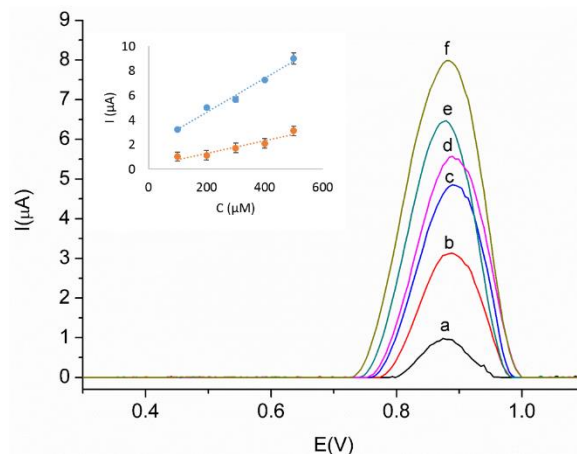


**Figure 8.** SW voltammograms of cocaine at MIP-sensor in PBS pH 11.0 at various concentrations (a) 50  $\mu\text{M}$  (b) 100  $\mu\text{M}$  (c) 200  $\mu\text{M}$  (d) 300  $\mu\text{M}$  (e) 400  $\mu\text{M}$  (f) 500  $\mu\text{M}$ . Inset: calibration line for MIP ( $\bullet$ ) and NIP ( $\square$ ) sensor, in the range 100-500  $\mu\text{M}$ .

To evaluate the reproducibility of the MIP-sensor three distinct electrodes were subjected to SWV measurements of 300  $\mu\text{M}$  cocaine solution in PBS pH 7.0 under optimized conditions. The relative standard deviation was 1.89%. To check the stability the MIP-sensor was stored at room temperature for 28 days, after which the signal of cocaine decreased to 92.6% of the original signal, showing that the film has long-term stability.

#### Selectivity

The selectivity of the MIP sensor to cocaine and homatropine, an alkaloid with similar structure to cocaine was assessed. Homatropine shows an oxidation peak on bare GPH around 0.85 V at pH 11.0, probably through a similar mechanism as cocaine – oxidation of tertiary amine. Upon incubation of MIP electrodes with 200  $\mu\text{M}$  homatropine solution pH 7.0 and SWV measurements at pH 11.0, no oxidation peak was observed demonstrating that homatropine does not bind to the MIP layer.

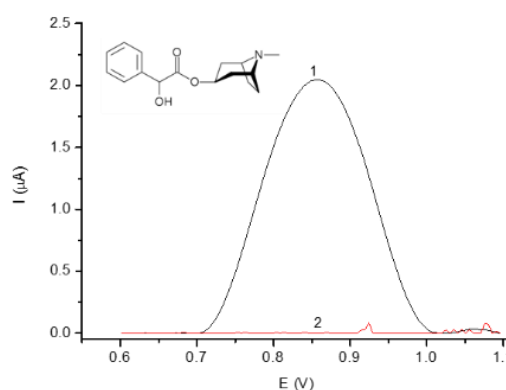


**Figure 9.** SW voltammograms of 200  $\mu\text{M}$  homatropine at bare GPH (1) and at MIP-sensor (2) in PBS pH 11.0. Scan rate 50 mV/s. Incubation time homatropine solution pH 7.0 at MIP-sensor 5 min, followed by 1 min wash with PBS pH 7.0.

### Real sample analysis

Saliva, river water and street samples were selected to assess the applicability of the MIP sensor for various real samples analyses. For saliva and river water the samples were prepared as described in section 2.1. of Materials and Methods and spiked with 100  $\mu\text{M}$  cocaine. The recovery values obtained for saliva and river water were 99.4% (RSD 13.2%) and 103.1% (RSD 6.3%), respectively.

To evaluate if the developed platform is suitable for screening of confiscated powders to detect the presence of cocaine, the MIP sensor was tested for the analysis of two street samples as described in Experimental section. SWV measurements revealed solely the oxidation peak of cocaine, demonstrating that the MIP films are selectively binding cocaine and are thus suitable for screening of drug street samples.

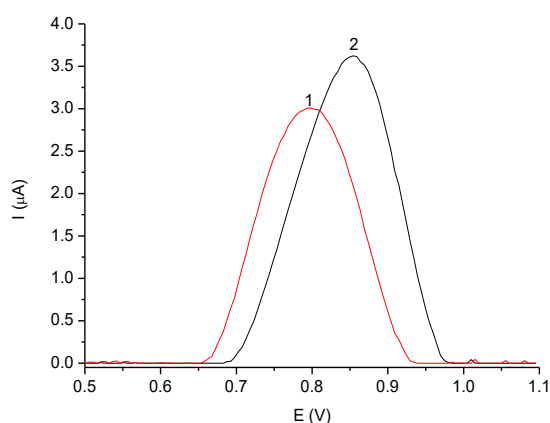


**Figure 10.** SW voltammograms obtained for two real street samples with the MIP-sensor. Numbers 1 and 2 correspond to the samples 1 and 2 described in Experimental section.

### Conclusions

In this work, a sensing platform based on selective MIP layers for direct cocaine detection by SWV was developed. The selective MIP-layer was readily prepared by electropolymerization of PABA in the presence of cocaine onto PdNPs modified GPH-SPE. Molecular modeling studies were useful to select PABA as appropriate monomer with high affinity for cocaine. A detection limit of 50  $\mu\text{M}$  was achieved in standard solutions with the new MIP-sensor. The sensor showed good stability, reproducibility and selectivity, and was successfully applied for the detection of cocaine in complex matrices, such as saliva, river water and street samples. The sensitivity of the MIP-based sensor is not low enough for applications on biological samples without any preconcentration step, however is sufficient for the identification of cocaine in street samples. Hence, the novel MIP-based sensor is a promising tool for police investigations.

### Conflicts of interest

There are no conflicts to declare.

### Acknowledgements

This project has received funding from the European Union's Horizon 2020 research and innovation programme under the Marie Skłodowska-Curie Grant Agreement No. 753223 Narcoreader.

### References

- 1 EU drug markets report, in-depth analysis, 2016, EMCDDA, Europol. [http://www.emcdda.europa.eu/publications/joint-publications/eu-drug-markets-2016-in-depth-analysis\\_en](http://www.emcdda.europa.eu/publications/joint-publications/eu-drug-markets-2016-in-depth-analysis_en) Accessed on 5/11/2018
- 2 J. Takitane, V. Leyton, G. Andreuccetti, H. Gjerde, T. Berg, *Forensic Science International*, 2018, **289**, 165.
- 3 A.L.N. van Nuijs, B. Pecceu, L. Theunis, N. Dubois, A. Covaci, *Environmental Pollution*, 2009, **157**, 123.
- 4 A. Florea, M. de Jong, K. De Wael, *Current Opinion in Electrochemistry*, 2018, **11**, 34.
- 5 L. Shaw, L. Dennany, *Current Opinion in Electrochemistry*, 2017, **1**, 23.
- 6 L. Poltorak, E.J.R. Sudhölter, M. de Puit. *TrAC Trends in Analytical Chemistry*, 2019, **114**, 48.
- 7 S. Komorsky-Lovric, I. Galic, R. Penovski, *Electroanalysis*, 1999, **11**, 120.
- 8 L. Asturias-Arribas, M.A. Allonso-Lomillo, O. Dominguez-Renedo, M.J. Arcos-Martinez, *Analytica Chimica Acta*, 2014, **834**, 30.
- 9 M. de Jong, A. Florea, J. Eliaerts, F. Van Durme, N. Samyn, K. De Wael, *Analytical Chemistry*, 2018, **90**, 6811.
- 10 M. de Jong, N. Slegers, J. Kim, F. Van Durme, N. Samyn, J. Wang, K. De Wael, *Chemical Science*, 2016, **7**, 2364.
- 11 M. de Jong, A. Florea, A.M. de Vries, A.L.N van Nuijs, A. Covaci, F. Van Durme, J.C. Martins, N. Samyn, K. De Wael, *Analytical Chemistry*, 2018, **90**, 5290.
- 12 R. Oueslati, C. Cheng, J. Wu, J. Chen, *Biosensors and Bioelectronics*, 2018, **108**, 103.
- 13 A. Mokhtarzadeh, J.E.N. Dolatabadi, K. Abnous, M. de la Guardia, M. Ramezani, 2015, **68**, 95.
- 14 K. Abnous, N.M. Danesh, M. Ramezani, S. M. Taghdisi, A.S. Emrani, 2016, **224**, 351.
- 15 P. Hashemi, H. Bagheri, A. Afkhami, Y.H. Ardakani, T. Madrakian, *Analytica Chimica Acta*, 2017, **996**, 10.
- 16 M. Majdinasab, A. Hayat, J.L. Marty, *TrAC Trends in Analytical Chemistry*, 2018, **107**, 60.
- 17 J.L. He, Y.F. Yang, G.L. Shen, R.Q. Yu, *Biosensors and Bioelectronics*, 2011, **26**, 4222.
- 18 M. Roushani, F. Shahdost-fard, *Materials Science and Engineering: C*, 2016, **61**, 559.
- 19 D.W. Zhang, F.T. Zhang, Y.R. Cui, Q.P. Deng, S. Krause, Y. L. Zhou, X.X. Zhang, *Talanta*, 2012, **92**, 65.
- 20 J. Gooch, B. Daniel, M. Parkin, N. Frascione, 2017, **94**, 150.
- 21 B. Yang, C. Fu, J. Li, G. Xu, *TrAC Trends in Analytical Chemistry*, 2018, **105**, 52.
- 22 K. Smolinska-Kempisty, O. Sheej Ahmad, A. Guerreiro, K. Karim, E. Piletska, S. Piletsky, *Biosensors and Bioelectronics*, 2017, **96**, 49.
- 23 M. Paredes-Ramos, F. Bates, I. Rodriguez-Gonzales, J.M. Lopez-Vilarino, *Materials Today Communications*, 2019, in press, <https://doi.org/10.1016/j.mtcomm.2019.05.002>
- 24 F. Bates, M.C. Cela-Pérez, K. Karim, S. Piletsky, J.M. López-Vilariño, *Macromolecular Bioscience*, 2016, **16**, 1170.
- 25 E.V. Piletska, D. Pink, K. Karim, S.A. Piletsky, *Analyst.*, 2017, **142**, 4678.
- 26 F. Bates, M. Busato, E. Piletska, M.J. Whitcombe, K. Karim, A. Guerreiro, M. del Valle, A. Giorgetti, S. Piletsky, *Separation Science and Technology*, 2017, **52**, 1441.



- 27 T. Cowen, K. Karim, S. Piletsky, *Analytica Chimica Acta*, 2016, **936**, 62.
- 28 J. Sánchez-González, Á. Peña-Gallego, J. Sanmartín, A. María Bermejo, P. Bermejo-Barrera, A. Moreda-Piñeiro, *Microchemical Journal*, 2019, **147**, 813.
- 29 S.A. Piletsky, K. Karim, E.V. Piletska, A.P.F Turner, A. P. F., Day, C. J., Freebairn, K. W., Legge, C., *Analyst*, 2001, **126**, 1826.
- 30 M. Marc, T. Kupka, P.P. Wieczorek, J. Namiesnik, *TrAC Trends in Analytical Chemistry*, 2018, **98**, 6.
- 31 M. Niu, C. Pham-Huy, H. He, *Microchimica Acta*, 2016, **183**, 2677.
- 32 G. Fu, H. He, Z. Chai, H. Chen, J. Kong, Y. Wang, Y. Jiang, *Analytical Chemistry*, 2011, **83**, 1431.
- 33 M.R. Halhalli, E. Schillinger, C.S. A. Aureliano, B. Sellergren, *Chemistry of Materials*, 2012, **24**, 2909.
- 34 C. Zhu, G. Yang, H. Li, D. Du, Y. Lin, *Analytical Chemistry* 2015, **87**, 230.
- 35 X. Tan, Q. Hu, J. Wu, X. Li, P. Li, H. Yu, X. Li, F. Lei, *Sensors and Actuators B*, 2015, **220**, 216.
- 36 F. Wang, L. Zhu, J. Zhang, *Sensors and Actuators B*, 2014, **192**, 642.
- 37 J. Borowiec, R. Wang, L. Zhu, J. Zhang, *Electrochimica Acta*, 2013, **99**, 138.
- 38 J. Eliaerts, P. Dardenne, N. Meert, F. Van Durme, N. Samyn, K. Janssens, K. De Wael, *Drug testing and analysis*, 2017, **9**, 1480.
- 39 P. Sharma, A. Pietrzyk-Le, F. D' Souza, W. Kutner, *Analytical Bioanalytical Chemistry*, 2012, **402**, 3177.
- 40 A. Florea, T. Cowen, S. Piletsky, K. De Wael, *Talanta*, 2018, **186**, 362.
- 41 S. Tokonami, H. Shiigi, T. Nagaoka, *Analytica Chimica Acta*, 2009, **641**, 7.
- 42 L. Rassaei, M. Sillanpää, R.W. French, R.G. Compton, F. Marken, *Electroanalysis*, 2008, **20**, 1286.
- 43 L. Rassaei, F. Marken, M. Sillanpää, M. Amiri, C.M. Cirtiu, M. Sillanpää, *TrAc Trends in analytical chemistry*, 2011, **30**, 1704.